ICHE 2014, Hamburg - Lehfeldt & Kopmann (eds) - © 2014 Bundesanstalt für Wasserbau ISBN 978-3-939230-32-8

SToRM: A Model for Unsteady Surface Hydraulics over Complex Terrain

F.J.M. Simões
U.S. Geological Survey, Golden, CO, USA

ABSTRACT: A two-dimensional (depth-averaged) finite volume Godunov-type shallow water model developed for flow over complex topography is presented. The model is based on an unstructured cell-centered finite volume formulation and a nonlinear strong stability preserving Runge-Kutta time stepping scheme. The numerical discretization is founded on the classical and well established shallow water equations in hyperbolic conservative form, but the convective fluxes are calculated using auto-switching Riemann and diffusive numerical fluxes. The model's implementation within a graphical user interface is discussed. Field application of the model is illustrated by utilizing it to estimate peak flow discharges in a flooding event of historic significance in Colorado, U.S.A., in 2013.

Keywords: Flood hydraulics, Numerical model, Godunov scheme, Flood inundation, Flood modeling

1 INTRODUCTION

The hazards of flooding and their detrimental impacts are becoming more frequent and likely to increase, as a consequence of higher sea level and intensifying cyclonic weather and precipitation suggested by current climate change science and research predictions (http://www.ipcc.ch/report/ar5/wg2/). The need to cope with flooding effects—such as flood-plain regulations, insurance, mitigation engineering works, and emergency preparedness—requires tools that can be used to provide quality predictions of flood timing, duration, and extent. A numerical flow model that solves the shallow water equations (SWEs) and simulates the hydrodynamics of a wide variety of surface flows will be a significant asset in the gamut of tools available to engineers, managers, and all decision makers involved in floodplain management. Such a model needs to be accurate, robust, efficient, and be available in a computer environment that facilitates data processing and analysis to reduce project turnaround time.

In recent years, Godunov-type schemes using a cell-centered finite volume formulation have become popular for solving the SWEs. This can be attributed to the ability of these schemes to deal with the most complicated shallow water phenomena, such as hydraulic jumps, flow regime change, and the wet-dry interfaces encountered in fast moving catastrophic flooding flows. SToRM (System from Transport and River Modeling) is a model that employs these techniques in two-dimensional (2D) unstructured grids, and that is contained in a graphical user environment that provides a number of tools to expedite its use by trained operators.

The purpose of this article is to provide a brief presentation of the model SToRM, and its implementation in a graphical user interface (GUI). Even though SToRM uses algorithms that are robust and general enough for application in a wide range of environmental hydraulics problems, it is applied here to estimate flood flow rates in a section of the historic flooding that occurred in Colorado,USA, in September of 2013.

2 MODEL DESCRIPTION

The model SToRM is based on the classical SWEs written in the conservative form:

$$\frac{\partial \boldsymbol{U}}{\partial t}+\frac{\partial \mathbf{F}(\mathbf{U})}{\partial x}+\frac{\partial \mathbf{G}(\mathbf{U})}{\partial y}=\mathbf{S}(\mathbf{U}) \tag{1}$$

$$\mathbf{U}=\begin{bmatrix} h \\ hu \\ hv \end{bmatrix}, \mathbf{F}=\begin{bmatrix} hu \\ hu^2+gh^2/2 \\ huv \end{bmatrix}, \mathbf{G}=\begin{bmatrix} hv \\ huv \\ hv^2+gh^2/2 \end{bmatrix}, \mathbf{S}=\begin{bmatrix} 0 \\ gh(S_{0x}-S_{fx}) \\ gh(S_{0y}-S_{fy}) \end{bmatrix}$$

where t is time, h is the water depth, g is the acceleration due to gravity, u and v are the depth-averaged flow velocities in the x and y Cartesian directions, S_0 is the bed slope, and S_f is the bottom friction. Integrating eq. (1) over a standard control volume Ω and applying the divergence theorem results in

$$\frac{\partial}{\partial t}\int_{\Omega}\mathbf{U}d\Omega+\oint_{\partial\Omega}(\mathbf{E}\cdot\mathbf{n})\,ds=\int_{\Omega}\mathbf{S}d\Omega \tag{2}$$

where $\mathbf{E} = (\mathbf{F},\mathbf{G})^{\mathrm{T}}$ and $\mathbf{n}$ is the outward-pointing unit vector normal to the control volume boundary $\partial\Omega$. SToRM is based on the numerical integration of eq. (2) over cell-centered, non-overlapping triangles:

$$\frac{\partial\Omega_i\mathbf{U}_i}{\partial t}=\sum_{k=1}^{3}\mathbf{E}_{ik}\Delta l_{ik}+\mathbf{S}_i\Omega_i \tag{3}$$

In eq. (3), $\mathbf{U}_i$ are the average values of the conserved variables over triangle i, $\mathbf{E}_{ik}$ are the inviscid fluxes through triangle edge k, Δl_{ik} is the length of edge k, $\mathbf{S}_i$ contains the source terms, and Ω_i is the triangle's area.

Following the principles of Godunov-type methods, the inviscid fluxes $\mathbf{E}_{ik}$ are numerical fluxes arising from a local Riemann problem at each triangle edge. Here, $\mathbf{E}_{ik}$ are computed using Roe's flux function at those edges (Roe, 1981):

$$\mathbf{E}_{ik}=\tfrac{1}{2}[(\mathbf{E}_{ik}^{+}+\mathbf{E}_{ik}^{-})-\boldsymbol{\Gamma}(\mathbf{U}_{ik}^{+}-\mathbf{U}_{ik}^{-})]$$

where the '+' quantities are reconstructed at the midpoint of the edge k using data from control volume i and the '-' quantities are reconstructed using data from the adjacent control volume. In SToRM, the upwinding factor $\boldsymbol{\Gamma}$ can be computed in one of two manners: (1) as in the algorithm of Alcrudo and Garcia-Navarro (1993)—augmented with the entropy fix of Harten and Hyman (1983)—or (2) by using Rusanov's (1961) numerical flux. The first approach is more computational demanding (i.e., it requires more computer number crunching), but it has the shock capturing properties needed to compute the flow at discontinuities such as hydraulic jumps and wet-dry fronts, whereas the latter is computationally much simpler and less demanding, but may introduce spurious numerical diffusion into the solution. The decision of which to use is done at each triangle edge: if $|h^+ - h^-|/\mathrm{Max}\{h^+,h^-\} > \delta_s$ then Alcrudo and Garcia-Navarro's method is used, otherwise Rusanov's method is used. δ_s is a threshold value used to detect discontinuity across element edges and is usually set to 0.1%, a value found by numerical experimentation.

Second-order accuracy is achieved using a piecewise linear model for the cell variables with the usual MUSCL reconstruction, with limiting to enforce monotonicity near sharp gradients and discontinuities of the dependent variables. The continuously differentiable limiter by Venkatakrishnan (1995) is chosen because it avoids introducing discontinuities to the computation of the reconstructed function and, consequently, to the fluxes, therefore improving the convergence properties of the solver over other commonly used discontinuous limiters. Computation of the gradients is done using a second-order-accurate least-squares technique conditioned by the use of inverse distance weighting.

The friction terms are discretized in a semi-implicit manner:

$$q_{xi}^{n}=\frac{\hat{q}_{xi}^{n}}{1+g\Delta t\hat{S}_{fxi}^{n}/\hat{u}_{i}^{n}},\quad q_{yi}^{n}=\frac{\hat{q}_{yi}^{n}}{1+g\Delta t\hat{S}_{fyi}^{n}/\hat{v}_{i}^{n}}$$

where $q_x = hu$ and $q_y = hv$ are the components of the unit discharge, the superscript n refers to the time step, and the variables with a hat are frictionless-computed quantities. This discretization avoids numerical oscillations in regions of high friction and low water depth, such as in wet-dry fronts, and impacts positively the conditional stability limits mentioned in the next paragraph.

The solution is advanced explicitly in time using nonlinear Strong Stability Preserving Runge-Kutta (SSPRK) schemes, also known as Total Variation Diminishing (TVD) Runge-Kutta schemes (Gottlieb et al., 2001). This is done by first rewriting the governing equations, eqs. (3), as a coupled system of ordinary differential equations:

$$\Omega_i \frac{\partial q_i}{\partial t} = R_i(u, v; t), \qquad i = 1,2,3 \tag{4}$$

where R_i is called the residual. Here, a simplified form of the SSPRK schemes is used, in which a m-stage SSPRK method for eq. (4) is written in the form

$$\begin{cases} u^{(0)} = u^n \\ u^{(i)} = \sum_{j=0}^{i-1} \alpha_{ij} u^{(j)} + \beta_i \frac{\Delta t}{\Omega_i} R\left(u^{(i-1)}\right), \ \alpha_{ij} \geq 0, \quad i = 1, \dots, m \\ u^{n+1} = u^{(m)} \end{cases}$$

where Δt is the time step size, the superscripts n and $n + 1$ denote the time level, and the parenthetic superscripts denote the Runge-Kutta level. The coefficients α and β are chosen to meet desired criteria. SToRM implements three optimal (in the sense of the Courant-Friedrichs-Lewy CFL stability coefficient θ) SSPRK schemes: first order ($m = 1$), second-order ($m = 2$), and third-order ($m = 3$). These schemes are all subjected to the same stability criterion and have an upper bound for θ. For time-dependent cases, the time step Δt is either prescribed or computed from

$$\Delta t = \theta \mathrm{Min} \left\{ \frac{l_k}{\lambda_k^*} \right\}_{k=1,\dots,N}$$

where l_k is the length of triangle edge k, λ^*_k is the highest eigenvalue at the edge's midpoint, and N is the number of fully wet edges over the entire computational domain. In the latter case, θ must be prescribed.

Boundary conditions are applied at the edges of the model grid using Riemann invariants, i.e., the boundary fluxes are also computed by solving a Riemann problem between the interior states and the "ghost" states outside the computational domain. These "ghost" states are introduced in order to compute the boundary fluxes in a similar and consistent way to the interior fluxes. Here, an approach identical to that of Anastasiou and Chan (1997) is used for solid walls, inflow, and outflow boundaries. However, wetting and drying fronts require a separate treatment.

Wetting and drying occurs not only during the propagation of floods, but also at the edges of any body of water. Thus, the dry-wet front constitutes not only a propagation problem, but also a static boundary condition problem, because it defines the shoreline. It is not easy to include these effects in a straightforward manner in a numerical code and most researchers resort to different degrees of approximation. Advancing wet-dry fronts are treated with the method of Brufau et al. (2002), which uses a numerical flux that can be applied to zero-depth cells and that maintains the C-property. The key concept is that the fluxes at the advancing front must be determined from the wet side of the front: the velocity at the cell boundaries separating wet and dry states is determined from the wet side, and the interface flux only uses the information coming from the wet side. This procedure allows including wetting and drying fronts in the ordinary cell flux computations without requiring the artificial wetting of dry cells. Drying fronts pose the additional problem that, during a drying time step, negative water depths may be reached. Mass conservation requires that the time step should be restricted to the value that corresponds to the time that takes the cell to dry out, i.e., to reach $h_i = 0$. SToRM performs additional checks and adjustments to ensure that mass is conserved at every time step without imposing these constraints to the time step size. These checks and adjustments are presented with greater detail in Simões (2011).

The shoreline treatment is different from the two preceding cases. A shoreline is defined when all the surrounding dry triangles of a partially or fully wet control volume have a mean bed elevation higher than the stage at the centroid of the triangle. Under this circumstance the shoreline is defined at the control volume edges and is also subjected to a special treatment. Partially wet triangles have corrections applied to their wetted area and water depth. The treatment is different whether drying or wetting is occurring. The interested reader is referred to Simões (2011), where detailed descriptions and validations of the methods are presented.

3 INTEGRATION IN A GUI

Integration of a numerical model within a graphical framework allows bridging the gap between model development and model use, and encourages model dissemination and application. One such framework developed specifically for environmental flow modeling is the iRIC Project (http://i-ric.org/en/), which provides a means to integrate diverse models within the same GUI, using the same data formats and protocols. The iRIC framework provides operational facilities that are model independent, such as data input and output (multiple formats are supported), automatic grid generation (provided by the two-dimensional grid generator and Delaunay triangulator of Shewchuk, 2002), interactive visualization and editing of model input and output, ability to work with ancillary data sets for model calibration, and device-independent plotting. This functionality frees the numerical model from all of these concerns by separating the roles of model developer from those of GUI programmer, with consequential benefits to both.

A schematic view of how the SToRM model is integrated in the iRIC graphical framework is given in Fig. 1. A graphical user interface is used to receive user input and to plot data. The GUI communicates with SToRM through a device-independent file using a format that has become a standard in many applications of computational fluid dynamics (CGNS, see http://cgns.sourceforge.net/). SToRM runtime information can also be displayed in a console window. The model parameter definitions needed to customize the GUI to the specific requirements of SToRM are coded in a flat file in XML format (http://www.w3.org/XML/). The GUI can read data in a multitude of formats commonly used in hydraulics and other digital elevation modeling applications. Entire SToRM set-ups, including input data, parameter definitions, and model simulation output, can be saved in single data files for later use, and for transmission and archival.

The model SToRM is implemented within the iRIC GUI and can be freely downloaded from the official iRIC Project Web Site at http://i-ric.org/en/. The calculations presented in this work were obtained using version 2.2 of the iRIC distribution package.

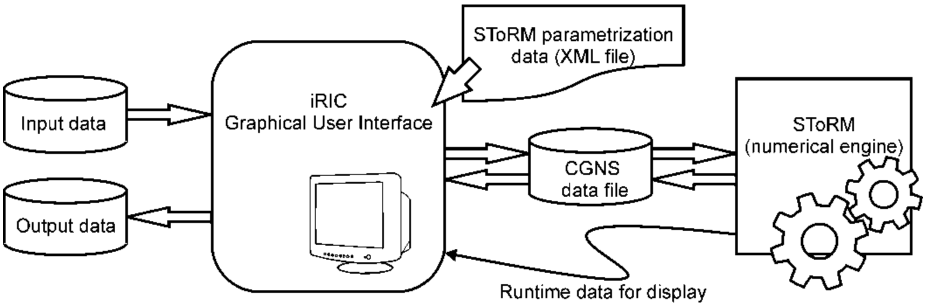

Figure 1. Schematic outline of the integration of model SToRM in the iRIC modeling framework. The CGNS data file contains computational grid, boundary condition data, model parameters, and complete numerical solutions obtained at multiple simulation times.

4 APPLICATION: ESTIMATING PEAK FLOODING FLOWS

In the week of September 9–15 of 2013, a slow-moving cold front clashed with warm monsoonal air over Colorado, causing unusually heavy rain that resulted in catastrophic flooding along a large extent of Colorado's Front Range. The flood waters spread from Fort Collins in the north, to Colorado Springs in the south over an area that extended for approximately 320 km (200 miles). Nearly 19,000 homes were damaged, with over 1,500 destroyed, and more than 11,000 people had to be evacuated, with eight dead and two more missing and presumed dead. It is estimated that at least 30 state highway bridges were destroyed and an additional 20 seriously damaged, with many miles of roads and freight and passenger rail lines significantly damaged or altogether washed out. Estimates of economic losses have surpassed $2 billion US Dollars (Novey, 2013).

Due to the high discharges and water depths that occurred in many of the affected streams, some of the US Geological Survey gaging stations were submerged or completely destroyed, precluding direct measurement of river stage at those locations. Such was the case at the confluence of the St. Vrain Creek and Boulder Creek near the city of Longmont, northwest of Denver, CO. As a result of high flows, the USGS Gaging Station 06725450 (http://waterdata.usgs.gov/co/nwis/uv/?site_no= 06725450), located at St. Vrain Creek at Highway 119 (HWY 119), was destroyed and failed to record the stage at the peak of the flood. No high water marks were collected at this location during the later forensic work related to this flood, therefore preventing the realization of an indirect measurement of the peak flow. This section describes the application of model SToRM to estimate the peak discharge passing at the gaging station and over HWY 119, which had a section over 1.7 km (1 mile) long under water.

The principal factor determining the choice of the methods used to accomplish the objective of this study is the availability of data—or, to be more precise, the lack thereof. In particular, the absence of high water marks makes it difficult, or impossible, to use conventional indirect estimation methods. The problem is compounded by the local topography, where two streams merge into a single branch, therefore further limiting the amount of hydraulic and hydrologic techniques that can be employed usefully in this region.

The data sets available for this work consist of topographic data and flood delineation data. The topography was taken from USDA Geospatial DATA Gateway (http://datagateway.nrcs.usda.gov/), which is from pre-flood USGS national elevation data (NED) at 1/9 arc-second resolution, i.e., with a spatial resolution of 3 meters. There was no post-flood LiDAR data for the site at the time of this study. Flood delineation data were obtained from remote sensing and are available as breaklines containing the discretized delineation of the flood extents in the area of interest (Chris Cole, USGS, Personal Comm., April 23, 2014). The model was set up to represent an area of 5 km (3.1 miles, east to west) by 4.5 km (2.8 miles, north to south) centered at the USGS Gaging Station 06725450, placing the model's inflow boundaries about 2.5 km (1.6 miles) upstream from the gaging station, and the outflow boundary 2.5 km (1.6 miles) downstream from it, as illustrated in Fig. 2. This design places these boundaries away from the area of interest, therefore insulating it from imprecisions due to approximate representation of the water surface elevation at the downstream end, and of synthesized velocity distributions at the upstream boundaries. The outflow boundary was set at St. Vrain Creek at HWY 25 (Interstate 25), because it is known that HWY 25 did not get flooded, and knowing that the flow was contained within the bridge opening permitted setting the boundary condition (i.e., water surface elevation under the bridge) close to that of the actual flood, which is near the invert of the bridge.

Figure 2. Aerial photograph of the modeled region (image source: The National Map, http:// http://nationalmap.gov/). The limits of the computational grid are given by the polygon shown. Note the inflowing tributaries at the south (Boulder Creek) and southwest (St. Vrain Creek) and the outflow boundary at the northeast (St. Vrain Creek). The circle marks the location of the USGS Gaging Station.

The model SToRM uses a spatial discretization based on triangles and the user interface iRIC provides an automatic grid generator that takes into account user input. User input is used to define grid shape and cell size, and is especially important in ensuring that topographic features of hydraulic relevance are discretized with the appropriate accuracy for model representation. Several discretization test runs were performed to determine the necessary degree of grid refinement. These tests compared the results obtained with different grid resolutions to determine the best working grid, i.e., the grid that provided the best computational performance without degrading the quality of the computed flood extents. A grid with 57,055 points (113,140 triangles) was constructed, representing a grid of triangles with a maximum area of 173.2 m^2 (1864 ft^2) each. The grid was selectively refined in certain regions, such as near the gaging station, and break lines were used to capture a number of significant terrain features.

To determine the value of the flow discharge at St. Vrain and Boulder Creeks, which is the objective of this study, the following trial-and-error procedure was followed:

1. Guess the discharge values for St. Vrain Creek and Boulder Creek.
2. Use the guessed discharges to configure a model run.
3. Run the model SToRM until steady state conditions are reached.
4. Compare the predicted inundation levels to the known flood delineation contours.
5. If the agreement between data and prediction is poor, guess new discharge values and return to step 2
6. Once the agreement between data and prediction is optimized, adopt the final discharge values as the final estimated discharge for each creek.

Surface roughness was guessed by judging the type of land use based on the analysis of aerial photography. There are many land uses in the modeled region, including residential, commercial, agricultural, gravel mining, and open space, and different roughness values were used to represent each, assigned from previous experience using the model SToRM in similar land surface textures. Each run was started from an initial state in which there was little or no flooding taking place, with the water mostly confined within channel banks. The model run progressed in an unsteady manner, where the inflows at St. Vrain and Boulder Creek were ramped to the desired guessed values and the computational domain was allowed to flood as if a flooding event was taking place. Once the hydrograph attained the desired high inflowing discharges, the run was sustained until steady state conditions were reached. This process does not represent the rate of flooding accurately, because the inflow hydrographs used do not represent the actual flooding event well, but it allows for the model to compute the actual flood extents without the need for any preconceived ideas about what the flood stages should look like.

In practice, a series of discharge guesses that under- and over-shoot the answer are used to perform model runs. The results of the model runs are compared to the known flood delineation contours and filed. A series of successive trials gradually hones the answer to the pair of values that provides the best possible agreement between the model predictions and the observations. In this study, the combination of values that provided the best agreement consisted of a discharge of 600 m^3/s (~21,000 ft^3/s) for St. Vrain Creek and a discharge of 250 m^3/s (~9,000 ft^3/s) for Boulder Creek, resulting in an estimated 850 m^3/s (~30,000 ft^3/s) passing through USGS Gaging Station 06725450 at HWY 119. The final results comparing model simulation and known flood delineation contours are shown in Fig. 3.

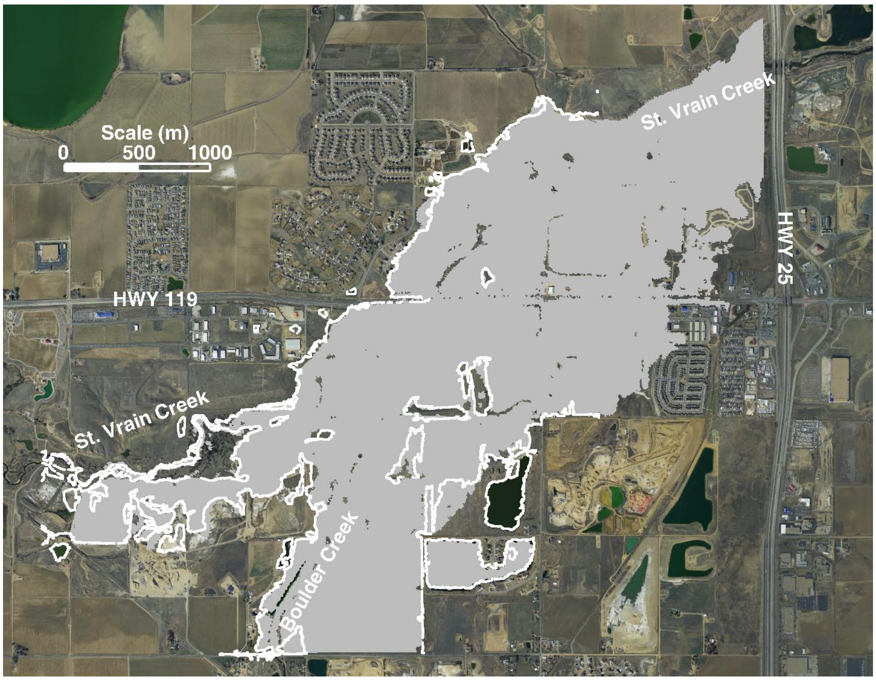

Figure 3. Comparison between observed flood delineation (white line) and predicted flooded area (gray area) on the same background image of Fig. 2. Note that the observed flood delineation contour does not extend all the way to the eastern part of the computational domain due to the absence of data.

5 DISCUSSION

The standard method of indirect measurement of discharge is based on matching the values predicted by a calculation method—such as a backwater procedure or Manning's equation—to high water marks collected *in situ* after the flood took place. An attempt was made to synthesize high water marks by intersecting the flood delineation contours with the DEM of the site to obtain the value of the water surface elevation at the edges of the flooded areas. High water marks can be constructed by using directly the water surface elevation values obtained from the intersection, or by interpolating them into the fully wetted areas by tracing cross sections and using the values at the edges. In practice, however, the wide extent of the flood and the complex topography of the flood plains made it difficult to trace hydraulically reasonable cross sections (lines normal to the flow direction that extend from left to right bank). For example, in many areas there were differences of more than one meter in water surface elevation between the left and the right margins, and the process of interpolating between such dissimilar values becomes highly speculative. To avoid introducing errors due to conjecture, it is a better approach to use data with the least amount of processing possible. Therefore, using a model to match directly the flood delineation lines offers a more effectual and well-grounded assault to the problem than the traditional methods of indirect measurement that use high water marks.

A depth-averaged two-dimensional flow model is used in this study, therefore fully three dimensional flow effects are not captured in the simulation. Some of the primary hypothesis used in the development of the model are that the vertical pressure distribution is hydrostatic, that momentum dissipation by the bottom stresses follows a quadratic drag law (in this study the Manning's friction coefficient was used), that there is no infiltration of water into the soil, and that there are no changes in bed topography during the flood, such as those that might result from flow induced bed erosion or sediment deposition. Although these are limiting assumptions, their use is appropriate and well justified in floods with the relative width and breadth encountered in this study, and there is an ample body of literature supporting it—see, for example, CFD (2005) and the references therein.

The source of data used introduces errors and uncertainties which are intrinsic to the type of data used to set-up the model and to evaluate the modeling results: topographic data and flood delineation contours, respectively. The process of delineating water boundaries from remote sensed images is challenging and its accuracy is influenced by river characteristics, neighboring land cover, and anthropogenic effects. There are many methods in use to accomplish the discretization of the delineation contours (Güneralp et al., 2014), but the accuracy of the resulting process is generally evaluated based on subjective visual assessment (Quackenbush, 2004), with larger uncertainties in areas of visual complexity. Another significant aspect concerns the time at which the remote imagery was acquired: for the purpose used in this study, it is important to use images taken at, or near, the peak of the flood. Unfortunately, with the USGS gage destroyed, the relation of the flood peak to the time at which the remote imagery was taken is unknown.

Topographic data are given by pre-flood USGS NED at 1/9 arc-second (3 meter) resolution. The accuracy of the NED varies spatially due to the variable quality of the different sources of DEM data. The overall absolute vertical accuracy of the USGS NED data has a root mean square error (RMSE) of 2.44 m (8 ft), (Gesch, 2007). However, information obtained from metadata in USGS NED data files for the Denver area from The National Map Viewer Web site (http://viewer.nationalmap.gov/viewer, accessed May 19, 2014) indicates that greater Denver DEM data were obtained from a Light Detection And Ranging (LiDAR) system and that the data acquisition occurred between March 15 and April 19, 2008. This increases the degree of vertical accuracy to a range of the RSME of 0.05–0.2 m (0.154–0.656 ft)(e.g., Baltsavias, 1999), but it also indicates that the data were approximately 5 ½ years old at the date of the flood; consequently any changes to the topography incurred in that period of time are not captured in the present study. Because part of the land has agricultural uses, it is expected that at least some change has taken place during this time, especially in the areas flooded by Boulder Creek.

Finally, there is the potential for operator error. In this study, operator error is introduced at the time when results are interpreted, which occurs when the final simulated flood contour lines are compared to the field data for the evaluation of the goodness of fit. Goodness of fit is evaluated by visual inspection of an image such as the one presented in Fig. 3. Although this is a generally acceptable method and is practiced by many, it lacks the objectivity of a mathematical criterion based on some type of computable measure. Such a criterion might be constructed from distance or area measures, such as the RMSE of the distance between the observed and the computed flood delineation contours, or from the area between the same two lines. At this point there is no published work about this subject and, therefore, there is no guidance about what types of criteria might be employed nor about the advantages of selecting one criterion over another. The development of a good goodness-of-fit criterion may be important if future work in this area is to be pursued, not only because it will allow removing the ambiguity introduced by a human operator, but also because it provides a necessary tool to streamline and automate the computational trial-and-error process developed and presented in the previous section.

6 CONCLUSION

A depth-averaged, two-dimensional model (SToRM) that solves the SWEs in unstructured triangular grids within the framework of the Godunov-type, cell-centered finite volume method, was briefly presented. The model was developed with the purpose of calculating unsteady flow over complex topography with wetting and drying moving fronts, such as those occurring in catastrophic flooding, and was applied to the estimation of the peak flow discharge passing at the USGS Gaging Station 06725450, near the city of Longmont, northwest of Denver, CO, during the historic flood event of September 2013.

Estimation of the peak discharge was accomplished by comparing the computed flood delineation contours with those obtained from remote sensed images. It was found that a close match was obtained when using a discharge of 600 m^3/s (~21,000 ft^3/s) for St. Vrain Creek and of 250 m^3/s (~9,000 ft^3/s) for Boulder Creek. It was noted, however, that these predictions are dependent on the accuracy of the data used: (1) the DEM data used by the model were sourced from USGS NED with a RMSE of 0.05–0.2 m (0.154–0.656 ft), and was 5 ½ years old at the time the flooding occurred; and (2) the flood delineation contours are subjected to uncertainties in areas of visual complexity and the source images must be obtained at peak flow, which may be an unknown by itself. Finally, the comparison between model predictions and field measurements was done by visual inspection, which introduces undesired operator ambiguity and underlines the need for the development of mathematical criteria that produce objective goodness-of-fit measures and that can be implemented in an automated computational procedure.

REFERENCES

Alcrudo, F., Garcia-Navarro, P. (1993). A high-resolution Godunov-type scheme in finite volumes in 2D shallow water equations, Int. J. Num. Meth. Fluids, Vol. 16, pp. 489-505.

Anastasiou, K., Chan, C.T. (1997). Solution of the 2D shallow water equations using the finite volume method on unstructured triangular meshes, Int. J. Num. Meth. Fluids, Vol. 24, pp. 1225-1245.

Baltsavias, E.P. (1999). Airborne laser scanning: basic relations and formulas, ISPRS J. of Photogramm. & Remote Sensing, Vol. 54, pp. 199-214.

Brufau, P., Vázquez-Cendón, M.E., Garcia-Navarro, P. (2002). A numerical model for the flooding and drying of irregular domains, Int. J. Num. Meth. Fluids., Vol. 39, pp. 247-275.

CFD (2005). Computational Fluid Dynamics, Applications in Environmental Hydraulics. P.D. Bates, S.N. Lane, R.I. Ferguson (Eds.), John Wiley & Sons, Chichester, England, 531 pages.

Gesch, D.B. (2007). Chapter 4–The National Elevation Dataset. In Maune, D. (Ed.). Digital Elevation Model Technologies and Applications: The DEM Users Manual, 2nd Edition: Bethesda, Maryland, American Society for Photogrammetry and Remote Sensing, pp. 99-118.

Gottlieb, S., Shu, C.-W., Tadmor, E. (2001). Strong stability-preserving high-order time discretization methods, SIAM Review, Vol. 43, No. 1, pp. 89-112.

Güneralp, I., Filippi, A.M., Hales, B. (2014). Influence of river channel morphology and bank characteristics on water surface boundary delineation using high-resolution passive remote sensing and template matching, Earth Surf. Process. Landforms, Vol. 37, pp. 977-986.

Harten, A. Hyman, J.M. (1983). Self adjusting grid methods for one-dimensional hyperbolic conservation laws, J. Comput. Phys., Vol. 50, pp. 235-269.

Novey, M. (2013). CDOT assessing 'millions and millions' in road, bridge damage. The Coloradoan, September 15, 2013.

Quackenbush, L.J. (2004). A review of techniques for extracting linear features from imagery, Photogramm. Eng. & Remote Sensing, Vol. 70, No. 12, pp. 1383-1392.

Roe, P.L. (1981). Approximate Riemann solvers, parameter vectors, and difference schemes, J. Comput. Phys., Vol. 43, pp. 357-372.

Rusanov, V.V. (1961). Calculation of intersection of non-steady shock waves with obstacles, J. Comput. Math. Phys. USSR, Vol. 1, pp. 267-279.

Shewchuk, J.R. (2002). Delaunay refinement algorithms for triangular mesh generation, Computational Geometry: Theory and Applications, Vol. 22, No. 1-3, pp. 21-74.

Simões, F.J.M. (2011). Finite volume model for two-dimensional shallow environmental flow, J. of Hydraulic Eng., ASCE, Vol. 137, No. 2, pp. 173-182.

Venkatakrishnan, V. (1995). Convergence to steady state solutions of the Euler equations on unstructured grids with limiters, J. Comput. Phys., Vol. 118, pp. 120-130.